In vivo role of ER-associated peptidase activity in tailoring peptides for presentation by MHC class Ia and class Ib molecules

Jingbo Yan,[1] Vrajesh V. Parekh,[1] Yanice Mendez-Fernandez,[1] Danyvid Olivares-Villagómez,[1] Srdjan Dragovic,[1] Timothy Hill,[1] Derry C. Roopenian,[2] Sebastian Joyce,[1] and Luc Van Kaer[1]

[1]Department of Microbiology and Immunology, Vanderbilt University School of Medicine, Nashville, TN 37232
[2]The Jackson Laboratory, Bar Harbor, ME 04609

Endoplasmic reticulum (ER)-associated aminopeptidase (ERAP)1 has been implicated in the final proteolytic processing of peptides presented by major histocompatibility complex (MHC) class I molecules. To evaluate the in vivo role of ERAP1, we have generated ERAP1-deficient mice. Cell surface expression of the class Ia molecules H-2K^b and H-2D^b and of the class Ib molecule Qa-2 was significantly reduced in these animals. Although cells from mutant animals exhibited reduced capacity to present several self- and foreign antigens to K^b-, D^b-, or Qa-1^b–restricted CD8$^+$ cytotoxic T cells, presentation of some antigens was unaffected or significantly enhanced. Consistent with these findings, mice generated defective CD8$^+$ T cell responses against class I–presented antigens. These findings reveal an important in vivo role of ER-associated peptidase activity in tailoring peptides for presentation by MHC class Ia and class Ib molecules.

CORRESPONDENCE
Luc Van Kaer:
luc.van.kaer@vanderbilt.edu

Abbreviations used: Endo H, endoglycosidase H; ERAP, ER-associated aminopeptidase; ES, embryonic stem; LCMV, lymphocytic choriomeningitis virus; Qdm, Qa-1 determinant modifier; TAP, transporter of antigen presentation.

MHC class I molecules present cytosolic peptides to class I–restricted CTLs. Shortly after their generation in the cytosol, peptides are translocated to the lumen of the ER by the transporter of antigen presentation (TAP) peptide transporter and loaded onto peptide-receptive MHC class I complexes with the assistance of a variety of chaperones, including calreticulin, ERp57, and Tapasin (1–4). Stably conformed and peptide-filled class I complexes then egress from the ER to the cell surface for recognition by CD8$^+$ T cells.

Most MHC class I allomorphs require peptides that are 8–10 amino acids in length for their stable assembly in the ER and transport to the cell surface (5). Therefore, cells must be capable of degrading the vast majority of intracellular proteins into peptides that meet this strict length requirement. Proteasomes appear to be responsible for the initial proteolytic attack of most proteins and defective translation products that are degraded in the cytosol (6–9). Purified proteasomes can generate peptides that are between 2 and 25 amino acids in length, but only ~15% of these peptides are of the correct size for optimal class I binding (10, 11). Although it has been well established that proteasomes are responsible for generating the final COOH terminus of peptide epitopes, they typically generate peptides with NH_2-terminal extensions (12). This tendency for generating precursors with NH_2-terminal extensions may be enhanced for a version of the proteasome, termed the immunoproteasome, containing catalytic subunits that are induced by IFN-γ (11, 12). These findings suggested that many peptides generated by the proteasome need to be trimmed, either before or after transport to the ER lumen, to the optimal length for binding with class I molecules. Recent studies have provided evidence for a role of both cytoplasmic and ER-resident proteases in trimming peptide precursors (9, 13, 14). Emerging evidence indicates that relatively long proteasome products (>15 amino acids in length) are shortened in the cytosol by the NH_2-terminal exopeptidase tripeptidyl peptidase II and that peptides with relatively short NH_2-terminal extensions may be further trimmed by cytosolic aminopeptidases and endopeptidases (13, 14). Although cytosolic peptidases

J. Yan and V.V. Parekh contributed equally to this work.

trim a substantial proportion of precursor peptides to the correct size for binding with class I, many peptides enter the ER lumen with NH_2-terminal extensions (15). This may be caused, at least in part, by the preference of TAP to translocate peptides between 8 and 16 amino acids in length (16). Although evidence for NH_2-terminal peptidase activity in the ER has been available for more than a decade (17, 18), the peptidases involved have eluded identification until recently (19–22). ER-associated aminopeptidase (ERAP)1, also called ER aminopeptidase associated with antigen processing, is a ubiquitous, IFN-γ–inducible metallopeptidase that catalyzes the sequential removal of diverse NH_2-terminal residues from peptide precursors (19–22). A second ER-resident, IFN-γ–regulated aminopeptidase, ERAP2, with more restricted tissue distribution, has been identified in humans but appears to be absent in rodents (22).

Apart from its inability to cleave the X-Pro (X denotes any amino acid) peptide bond, ERAP1 appears to have relatively little sequence selectivity (19, 22, 23). However, one striking and unique feature of ERAP1 is that it efficiently trims NH_2 terminally extended peptides but spares most peptides that are eight amino acid residues or shorter (20, 21, 24), suggesting that ERAP1 favors the generation of peptides that are of the optimal size for binding with class I. Nevertheless, in some cases, recombinant ERAP1 destroyed cognate peptide epitopes (20, 21). Consistent with these findings, reduction of ERAP1 expression by RNA interference resulted in defective presentation of several peptide epitopes (19, 21, 22) but did not affect or even enhance presentation of some other epitopes (19). Moreover, whether ERAP1 expression influences the levels of class I molecules displayed at the cell surface remains controversial. ERAP1 gene silencing in murine cells resulted in a reduction in the surface expression of H-$2K^k$ and H-$2L^d$ molecules (19), whereas ERAP1 silencing in human HeLa cells or ERAP1 overexpression in monkey COS cells had no effect on H-$2K^b$ cell surface expression (21). One group reported that ERAP1 silencing in HeLa cells resulted in an increase in HLA-A, HLA-B, and HLA-C surface expression (21), whereas another group found a modest reduction in HLA class I surface expression (22). The effects of ERAP1 silencing on the IFN-γ–induced expression of class I molecules are also controversial (21, 22).

The cell lines that have been used to study ERAP1 function likely express nonphysiological levels of antigen-processing factors that may impact the interpretation of the results obtained. For example, differences in the expression levels of ERAP2 among distinct HeLa cell lines have been observed (9). In addition, studies with RNA interference have intrinsic drawbacks that may complicate data interpretation (25). Moreover, cell lines do not permit analysis of ERAP1 function by professional APCs or to determine its role in the generation of CTL responses in vivo. As an approach to clarify these issues, we generated a mouse strain with a targeted disruption in the ERAP1 gene. Analysis of these animals indicated defects in the surface expression of class Ia and class Ib molecules, class I–restricted antigen presentation, and the generation of CTL responses. These findings reveal an important in vivo role of ERAP1 in optimizing peptides for surface display by MHC class I molecules.

RESULTS

Generation of ERAP1 mutant mice

ERAP1-deficient mice were generated by replacing a 600-bp fragment of the ERAP1 gene, containing the sequence encoding the putative active site of ERAP1, with a neomycin resistance cassette (Fig. 1, A–C). Absence of ERAP1 mRNA and protein in the mutant mice was confirmed by RT-PCR analysis (Fig. 1 D) and immunoblotting (Fig. 1 E), respectively. Because ERAP1 has been suggested to participate in several functions unrelated to antigen processing (26–28), we evaluated mice for obvious abnormalities. However, mice appeared healthy, were fertile, and we were unable to detect any obvious anatomical or developmental defects.

Impact of ERAP1 deficiency on class I cell surface expression

To evaluate the effects of ERAP1 deficiency on steady-state levels of MHC class I cell surface expression, we stained cells from wild-type and mutant animals with class I–specific antibodies. We found a reproducible reduction in the surface expression of H-$2K^b$ and H-$2D^b$ molecules on total mononuclear cells in the spleen, lymph node, and blood; on splenic DCs, T cells, and B cells (Fig. 2, A–C); and on fibroblast cell lines derived from these animals (Fig. 2 F). Levels of H-$2K^b$ and H-$2D^b$ were reduced ∼40 and 50%, respectively. We also found a significant reduction in the extent of surface display of the nonclassical class I (class Ib) molecule Qa-2 (∼35% reduction as compared with wild-type cells; Fig. 2, A–C), which is ubiquitously expressed and binds with a wide array of nonameric peptides (29, 30).

IFN-γ induces the transcription of MHC class I genes and a variety of antigen processing–related genes, including ERAP1 (13). Therefore, we measured class I levels on splenocytes and fibroblasts after treatment with IFN-γ. The results indicated similar but less pronounced differences in class I expression than those observed during steady-state conditions (Fig. 2, E and F). In fact, treatment of $ERAP1^{-/-}$ fibroblasts with IFN-γ for 5 d resulted in a profound increase in class I surface expression, reaching levels that were only slightly lower than those observed on similarly treated fibroblasts from $ERAP1^{+/+}$ mice (Fig. 2 F).

We also evaluated class I expression by Con A–activated spleen lymphoblasts, which showed less profound differences in class I surface expression between $ERAP1^{-/-}$ and $ERAP1^{+/+}$ cells than those observed during steady-state conditions (Fig. 2, A and D). Interestingly, however, the extent of surface display of another ubiquitously expressed class Ib molecule, Qa-1^b, which binds with a highly restricted set of nonameric peptides (31), was enhanced on lymphoblasts derived from ERAP1 mutant mice (∼30% increase as compared with wild-type cells; Fig. 2, A and D).

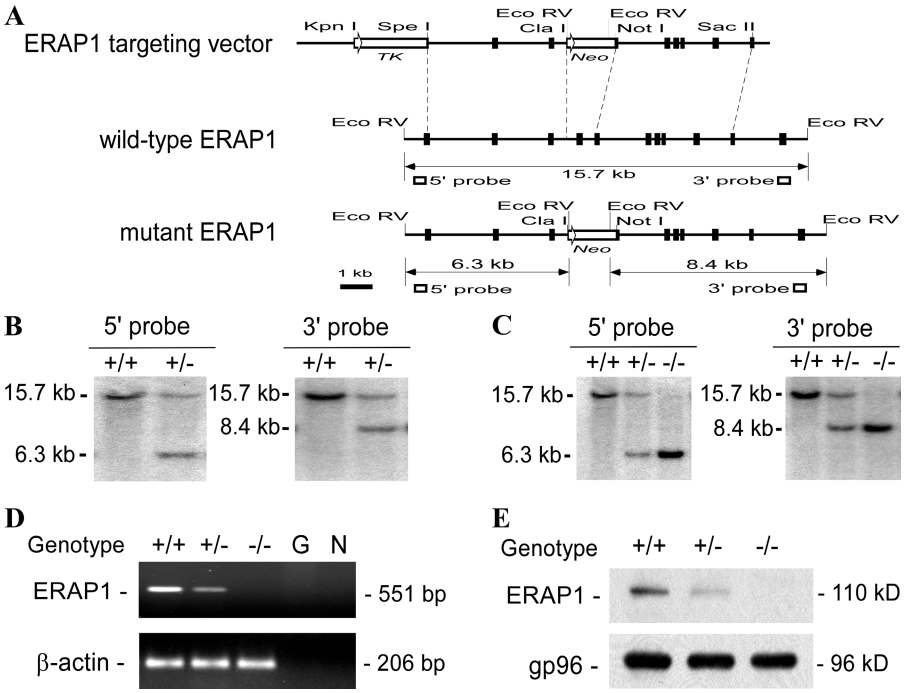

Figure 1. Generation of ERAP1 mutant mice. (A) The ERAP1 locus and targeting construct. Part of the wild-type ERAP1 gene is shown, along with the targeting construct, the mutated ERAP1 locus, and hybridization probes. Solid boxes indicate the exons of ERAP1. A 0.6-kb fragment, which contains the sequence encoding the Zinc-binding motif of the putative active site of ERAP1, was deleted and replaced with a neomycin resistance cassewwtte (Neo). The vector also contains a thymidine kinase (TK) cassette. ERAP1 5′- and 3′-flanking probes used for the screening of ES cell clones and mice are indicated, together with the expected sizes of the hybridizing restriction fragments in wild-type and mutant ERAP1 alleles. (B and C) Southern blot analysis of DNA from representative ES cell clones and mice. Genomic DNA was isolated from ES cell clones (B) and mouse tails (C) with the indicated genotype. DNA was digested with EcoRV and hybridized with the 5′ or 3′ probe (see A). (D) RT-PCR amplification of ERAP1 transcripts. Total RNA was isolated from the spleen cells of the indicated mice, reverse-transcribed, and amplified with ERAP1-specific primers. Genomic DNA (G) and water (N) were used as controls for DNA contamination and false positive amplification, respectively. β-actin mRNA amplification was used as a positive control. (E) Western blot analysis of ERAP1 expression. ER proteins isolated from the liver of the indicated mice were separated by SDS-PAGE and probed with anti-ERAP1 or anti-gp96 antiserum.

During these experiments we noted that heterozygous mutant animals expressed class I surface levels that were intermediate between wild-type littermates and homozygous mutant littermates (Fig. 2). These results suggested that ERAP1 expression levels in the ER are rate limiting for the generation of class I–binding peptides, at least in the absence of infection or IFN-γ production.

Class I maturation and stability

Next, we determined whether ERAP1 deficiency was associated with alterations in class I maturation and/or stability. The rate of transport of class I molecules from the ER to the cell surface can be estimated by the sensitivity of these molecules to attack by endoglycosidase H (Endo H), which cleaves sugar moieties from class I heavy chains before, but not after, glycan modifications in the medial Golgi apparatus. Pulse-chase experiments with spleen lymphoblasts from ERAP1$^{-/-}$ and ERAP1$^{+/+}$ mice revealed comparable acquisition of Endo H resistance by K^b and D^b heavy chains, whereas class I heavy chains from control TAP1$^{-/-}$ cells, expressing class I molecules that are largely retained within the ER (32), were profoundly defective in the acquisition of Endo H resistance (Fig. 3, A and B).

We evaluated the stability of class I heterodimers by incubating cell extracts prepared from metabolically labeled spleen lymphoblasts at different temperatures, followed by immunoprecipitation with conformation-dependent anti-K^b and -D^b antibodies. The results showed no detectable differences in this parameter between cells from ERAP1$^{-/-}$, ERAP1$^{+/-}$, and ERAP1$^{+/+}$ mice (Fig. 3, C and D).

As an additional measurement of class I stability, we treated splenocytes with brefeldin A to prevent transport of newly assembled class I complexes to the cell surface and determined the decay of H-2K^b and H-2D^b molecules with conformation-dependent antibodies. The results showed a significant increase in the decay of both surface K^b and D^b molecules from ERAP1$^{-/-}$ cells as compared with ERAP1$^{+/+}$ cells (Fig. 3 E). Nevertheless, the accelerated decay of class I molecules on ERAP1$^{-/-}$ cells was substantially less pronounced than on Tapasin$^{-/-}$ cells (Fig. 3 E), which express class I molecules that are predominantly loaded with low-affinity peptides (33–35).

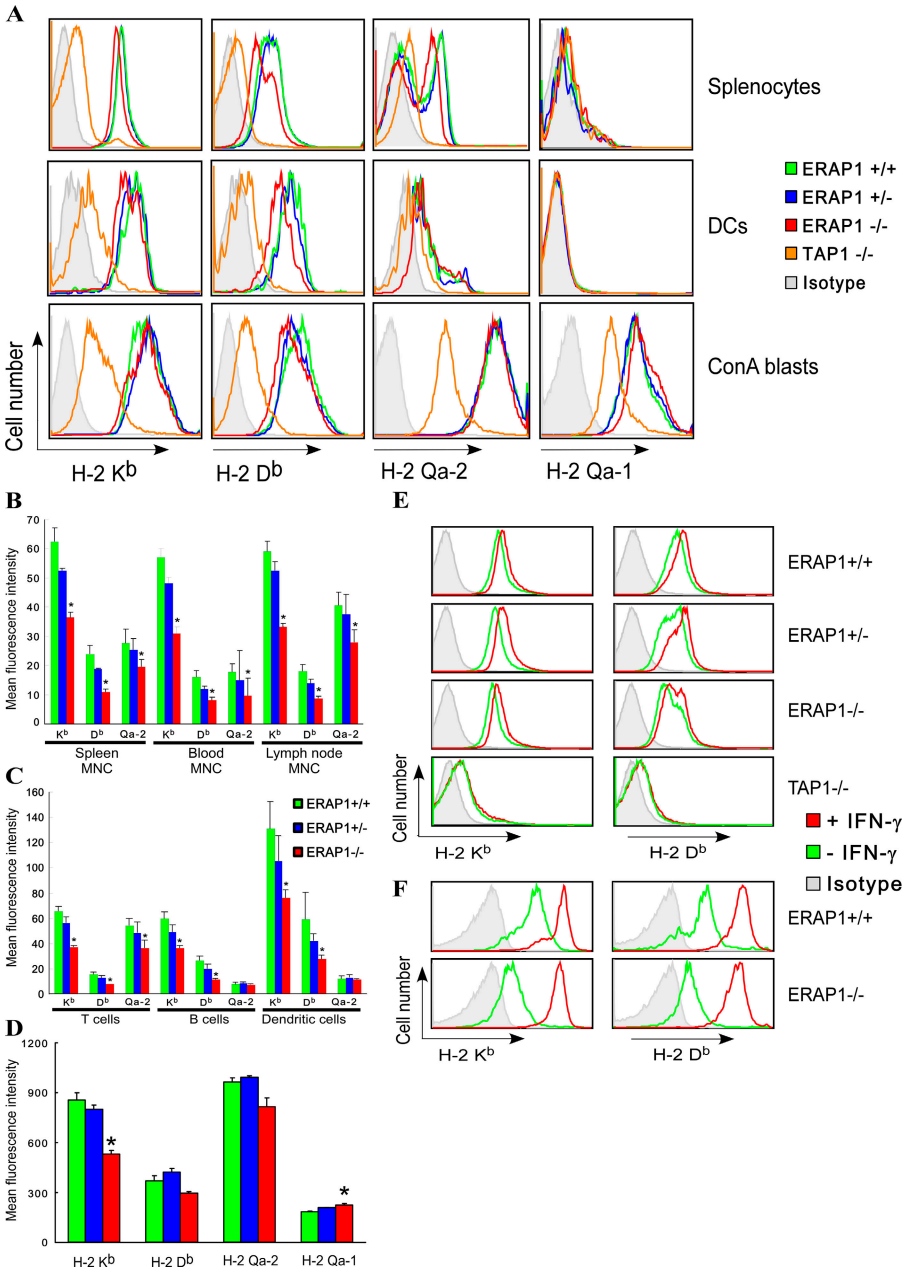

Figure 2. MHC class I cell surface expression. (A) Splenocytes, splenic DCs (B220^{-}CD11c^{hi}), or Con A–activated spleen lymphoblasts from the indicated mice were stained with antibodies directed against MHC class Ia (H-2K^{b} and H-2D^{b}) or class Ib (Qa-2 and Qa-1^{b}) molecules and analyzed by flow cytometry. (B–D) Summary of class I surface staining data. MHC class Ia and class Ib expression levels were analyzed on total mononuclear cells (MNC) from the spleen, blood, and lymph nodes (B), on splenic T cells, B cells, and DCs (C), or on Con A–activated spleen lymphoblasts (D). Results in B and C indicate the mean ± SE of five mice and results in D indicate the mean ± SE of three mice. *, $P < 0.05$. (E and F) IFN-γ–induced class I expression. (E) Spleen cells from the indicated mice were cultured with or without 15 ng/ml IFN-γ for 16 h, followed by staining with class I–specific antibodies and flow cytometry. One representative experiment of three is shown. (F) Ear fibroblast cell lines from the indicated mice were cultured with or without 15 ng/ml IFN-γ for 5 d, stained with class I–specific antibodies, and analyzed by flow cytometry.

Defective presentation of self-antigens

To determine the effects of ERAP1 deficiency on the presentation of self-antigens to class I–restricted CTLs, we evaluated the capacity of a panel of minor histocompatibility (H) antigen-specific CTL clones to react with splenocytes from wild-type and mutant animals. Because several of these CTLs recognize minor H antigens expressed in mice from the 129 but not C57BL/6 strain (36–38), in these experiments, we used mutant and wild-type animals on a homogeneous 129 strain–derived background (see Materials and methods). Results

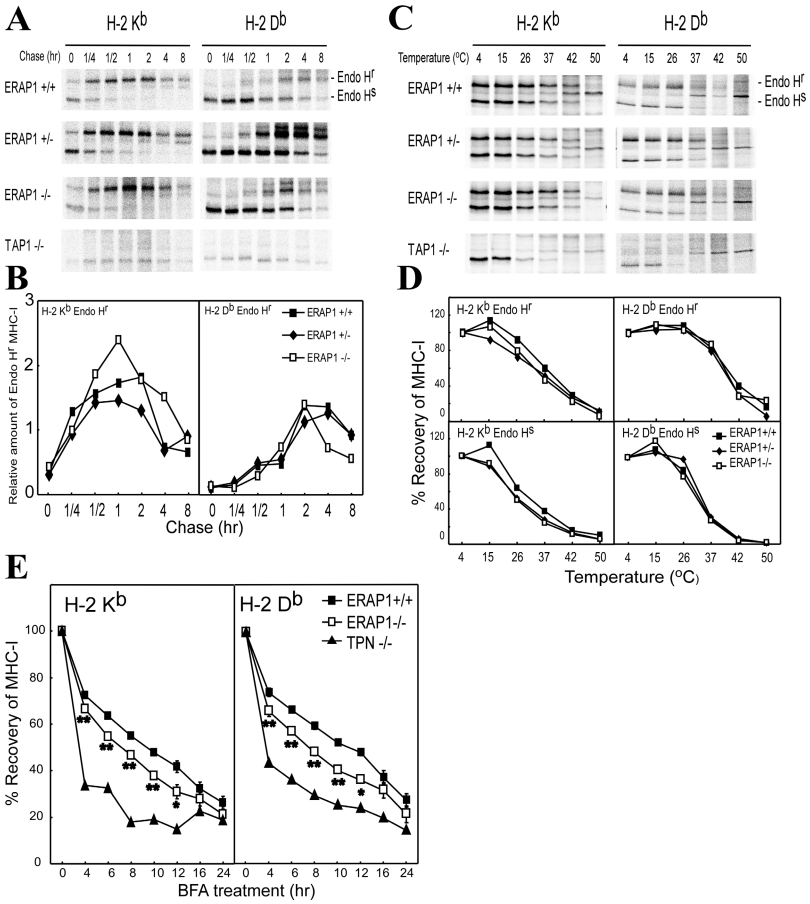

Figure 3. MHC class I maturation and thermostability. (A and B) Class I maturation. Con A blasts from the indicated mice were pulse-labeled with [^{35}S]methionine/cysteine for 10 min and chased at 37°C for the indicated times. Cell aliquots were lysed in NP-40 buffer. Class I molecules were precipitated with conformation-dependent antibodies (Y3 for H-2K^b and B22.249 for H-2D^b). Immunoprecipitates were treated with Endo H, resolved by SDS-PAGE, and developed by phosphorimaging (A). Endo H^r and Endo H^s forms of MHC class I are indicated. The band intensities of the Endo H^r forms of MHC class I glycoproteins were quantified by ImageQuant software. The relative amounts of mature MHC class I complexes are shown as mean absolute intensities of each band normalized against that of the Endo H^s band at time 0 in each experiment (B). One representative experiment of five is shown. (C and D) Class I thermostability in cell extracts. Con A blasts from the indicated mice were pulse-labeled with [^{35}S]methionine/cysteine for 1 h and chased at 37°C for 2 h. Cells were lysed in NP-40 buffer, aliquoted, and incubated at the indicated temperatures for 1 h. Class I molecules were precipitated with conformation-dependent anti–H-2K^b or anti–H-2D^b antibodies, followed by SDS-PAGE and phosphorimaging (C). The band intensities of Endo H^r and Endo H^s forms of MHC class I glycoproteins were quantified by ImageQuant software. Band intensities are shown as percent recovery of MHC class I complexes at different temperatures as compared with 4°C (D). One representative experiment of five is shown. (E) Thermostability of surface class I molecules. Splenocytes from ERAP1$^{-/-}$, ERAP1$^{+/+}$, and Tapasin$^{-/-}$ (TPN$^{-/-}$) mice were cultured at 37°C with brefeldin A (BFA) for the indicated time intervals and then stained with conformation-dependent anti–H-2K^b and anti–H-2D^b antibodies followed by flow cytometry. Results are presented as percent recovery of MHC class I expression at different time points as compared with the 0 time point. Results shown represent data for three ERAP1$^{-/-}$ mice, three ERAP1$^{+/+}$ mice, and one Tapasin$^{-/-}$ mouse. *, $P < 0.05$; **, $P < 0.01$.

showed a profound defect in the reactivity of two H60-specific CTL clones and of an HY-specific clone with 129.ERAP1$^{-/-}$ cells, whereas the two H4^b-specific clones reacted similarly with 129.ERAP1$^{-/-}$ and 129.ERAP1$^{+/+}$ cells, and an H13^b-specific clone reacted more strongly with 129.ERAP1$^{-/-}$ than 129.ERAP1$^{+/+}$ cells (Fig. 4 A). None of these clones reacted with cells from female C57BL/6 mice, whereas another clone, specific for the H4^a antigen, which is expressed in mice from the C57BL/6 but not 129 strain, reacted with cells from C57BL/6 mice but not with cells from 129.ERAP1$^{-/-}$ or 129.ERAP1$^{+/+}$ mice (Fig. 4 A). These findings indicated that ERAP1 expression can have a positive, neutral, or negative effect on antigen presentation.

We also investigated the capacity of a panel of Qa-1^b–restricted, alloreactive CTL clones to lyse spleen lymphoblasts from mutant animals. The results revealed modest but significantly reduced capacity of each of these clones to lyse mutant cells as compared with wild-type cells (Fig. 4 B). Subtle but reproducible differences in the extent of lysis of mutant cells, compared with wild-type cells, by distinct clones were observed, which is likely due to differences in the precise peptide selectivity of individual clones.

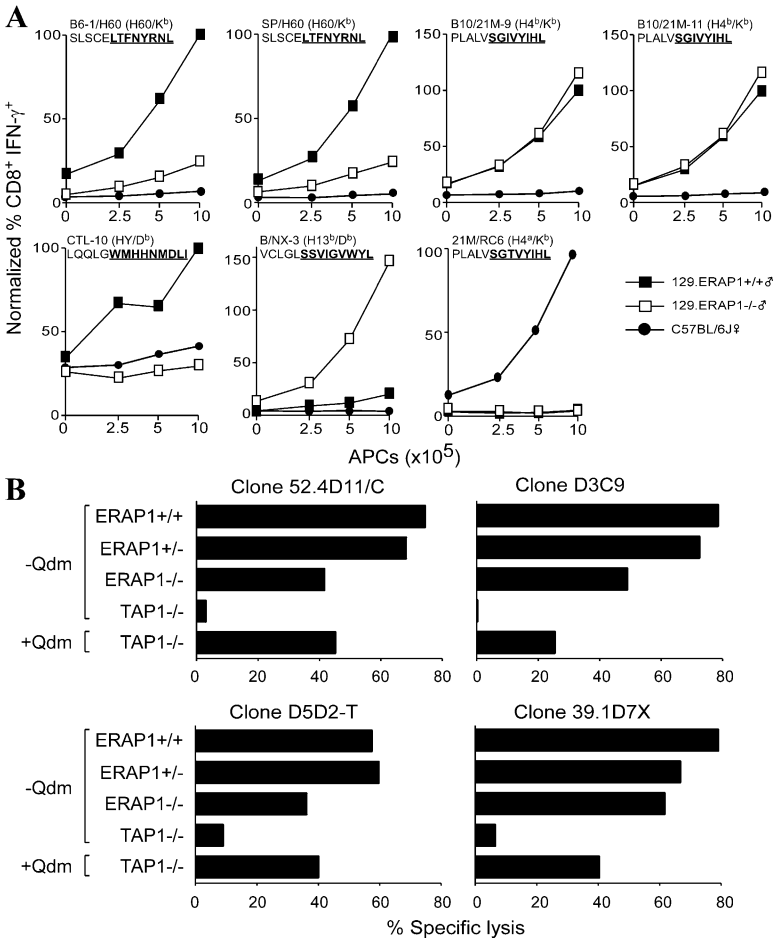

Figure 4. Presentation of self-antigens to class I–restricted CTLs. (A) Presentation of minor H antigens. The indicated numbers of spleen cells from male 129.ERAP1$^{+/+}$ mice, male 129.ERAP1$^{-/-}$ mice, and female C57BL/6 mice were used to stimulate the indicated minor H antigen–specific CTL clones for 6 h. CTL activation was evaluated by detection of intracellular IFN-γ among CD8$^+$ T cells. Data are plotted as the percentage of CD8$^+$IFN-γ$^+$ cells and normalized to the response to ERAP1$^{+/+}$ splenocytes. The class I allele and minor H specificity of individual CTL clones, together with the identity of their cognate peptide epitope (underlined) and a few NH_2-terminal flanking residues, are shown. Results are representative of five independent experiments for each clone. (B) Antigen presentation to alloreactive Qa-1^b–restricted CTLs. Con A blasts from the indicated mice were used as targets for the indicated Qa-1^b–restricted alloreactive CTL clones. TAP1$^{-/-}$ cells, pulsed with Qdm peptide, were used as a positive control. Results represent the mean from triplicate cultures at an effector–target ratio of 5:1. Results are representative of at least two independent experiments for each clone.

Defective presentation of foreign antigens

To investigate the impact of ERAP1 deficiency on the presentation of foreign antigens, we studied the capacity of mutant cells to display the immunodominant OVA-derived CTL epitope ($OVA_{257–264}$), after osmotic shock-mediated introduction of the native protein into the cytoplasm of cells, by H-2K^b molecules at the cell surface. H-2K^b/$OVA_{257–264}$ complexes were detected with an antibody that specifically reacts with this particular class I–peptide complex. Results demonstrated a profound defect of ERAP1 mutant cells in displaying K^b/$OVA_{257–264}$ complexes at the surface (Fig. 5 A). Staining levels of OVA-loaded ERAP1$^{-/-}$ cells were only slightly higher than OVA-loaded TAP1$^{-/-}$ cells, indicating a strict requirement of ERAP1 for generating this epitope, which is consistent with prior reports (19–21). Similarly, bone marrow–derived DCs and LPS-induced lymphoblasts from ERAP1$^{-/-}$ mice were defective in presenting OVA, introduced into these cells by osmotic shock, to an $OVA_{257–264}$-specific, H-2K^b–restricted T cell hybridoma (Fig. 5 B). Strikingly, cells from heterozygous mutant animals also exhibited profound defects in processing OVA for surface display by K^b (Fig. 5, A and B). Macrophages from mutant animals, infected with an OVA-expressing strain of *Listeria monocytogenes*, were also defective in presenting OVA antigens to $OVA_{257–264}$-specific T cells, but cells from heterozygous mutants behaved more similarly to cells from wild-type animals in this assay (Fig. 5 C).

We also tested the capacity of splenic DCs from mutant animals to cross-present OVA antigens, adsorbed to latex beads, to $OVA_{257–264}$-specific T cells. The results revealed a profound defect of ERAP1$^{-/-}$ DCs in cross-presenting OVA antigens (Fig. 5 D).

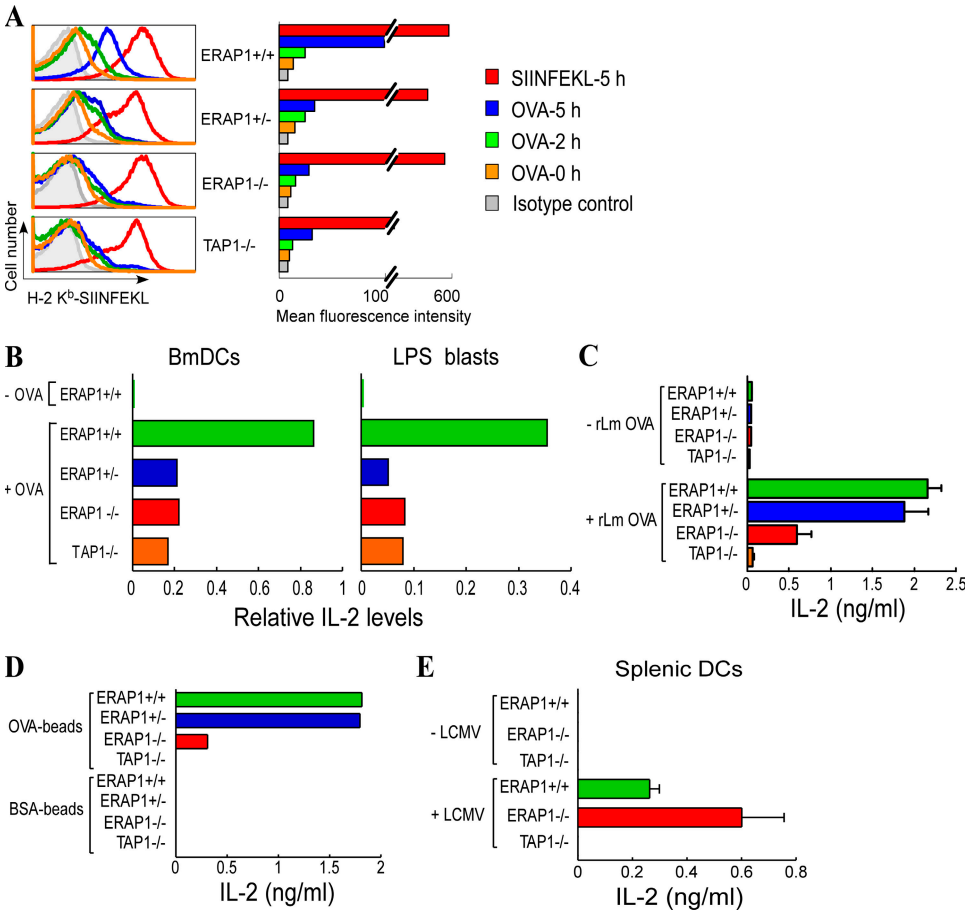

Figure 5. Presentation of foreign antigens to class I–restricted CTLs. (A–D) Processing and presentation of endogenous and exogenous OVA antigens. (A) Bone marrow–derived DCs (BmDCs) from the indicated mice were loaded with OVA by osmotic shock. Cells were incubated at 37°C for 0, 2, or 5 h and stained with the H-2K^b/SIINFEKL-specific antibody 25-D1.16 or an isotype control antibody followed by flow cytometry. SIINFEKL peptide-pulsed cells were used as a positive control. (B) Bone marrow–derived DCs or LPS-activated spleen lymphoblasts from the indicated mice were loaded with OVA as in A and cocultured with B3Z hybridoma cells overnight, followed by measurement of IL-2 in the supernatant. (C) Macrophages from the indicated mice were incubated in the absence or presence of OVA-expressing *L. monocytogenes* bacteria for 30 min and cultured with splenocytes from OT-1^{Tg}RAG1$^{-/-}$ mice for 24 h, and IL-2 production was assessed. (D) Splenic DCs from the indicated mice were incubated with BSA- or OVA-coated latex beads and cultured with splenocytes from OT-1^{Tg}RAG1$^{-/-}$ mice for 24 h, and IL-2 production was assessed. (E) Presentation of the immunodominant LCMV gp33 CTL epitope. Splenic DCs from the indicated mice were infected with LCMV and cultured with splenocytes from P14^{Tg}RAG2$^{-/-}$ mice for 24 h, and IL-2 production was assessed.

Finally, we infected DCs from wild-type and mutant animals with the lymphocytic choriomeningitis virus (LCMV) to compare the capacity of these cells to present the immunodominant glycoprotein-derived gp33 epitope to H-2D^b–restricted T cells. The results showed enhanced reactivity of the gp33-specific T cells with ERAP1$^{-/-}$ than ERAP1$^{+/+}$ cells (Fig. 5 E). These findings suggest that ERAP1 normally plays a role in destroying the LCMV gp33 epitope.

CD8$^+$ T cell development

The surface levels of MHC class I molecules and the diversity of peptides displayed by these molecules in the thymus can have a profound impact on both positive and negative selection of CD8$^+$ T cells (39). Therefore, we examined CD8$^+$ T cell development in ERAP1 mutant mice. Despite their reduced levels in MHC class I cell surface expression, the prevalence and numbers of CD8$^+$ T cells in ERAP1$^{-/-}$ mice were comparable to ERAP1$^{+/+}$ mice (Fig. 6 A and not depicted).

To determine whether ERAP1 deficiency influences the positive selection of individual TCRs, we examined CD8$^+$ T cell development in ERAP1$^{-/-}$ mice expressing a transgenic TCR (P14) specific for the gp33 peptide epitope derived from the LCMV glycoprotein. These studies were performed with transgenic animals on a RAG2-deficient background to enhance our capacity to detect defects in the positive selection of transgenic T cells. However, the results failed to reveal differences in the prevalence, numbers, or TCR expression levels among P14 TCR transgenic cells in ERAP1$^{-/-}$ versus ERAP1$^{+/+}$ mice (Fig. 6 B and not depicted).

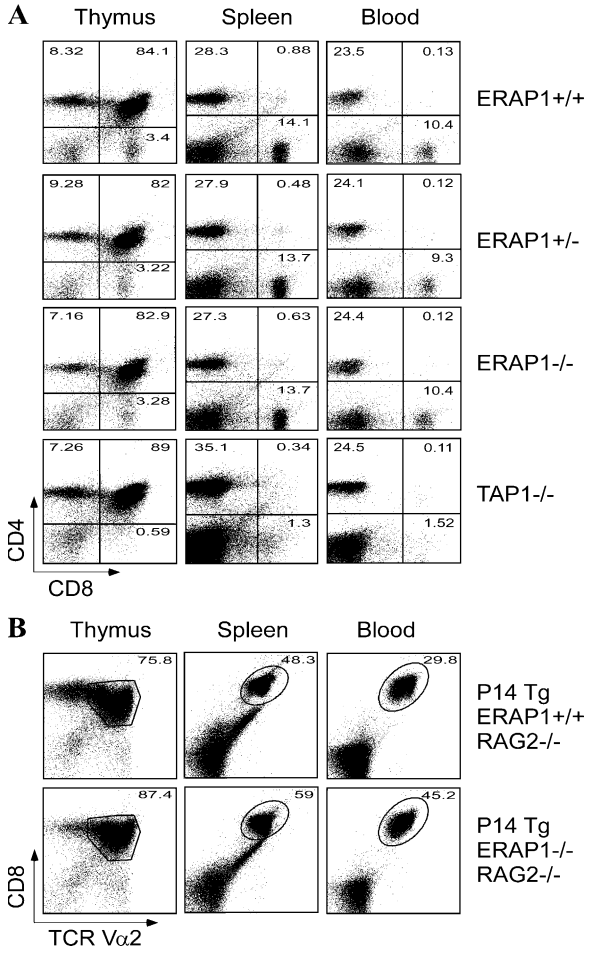

Figure 6. CD8⁺ T cell development. (A) Cells from the thymus, spleen, and peripheral blood of the indicated mice were stained with anti-CD4 and anti-CD8 antibodies and analyzed by flow cytometry. Numbers indicate the percentage of cells within each quadrant. (B) Development of P14 transgenic T cells. ERAP1$^{-/-}$ animals were bred with RAG2-deficient P14^{Tg} mice carrying a TCR specific for the LCMV gp33 epitope presented by H-2D^{b}. Cells from the thymus, spleen, and peripheral blood of P14^{Tg}ERAP1$^{-/-}$RAG2$^{-/-}$ and P14^{Tg}ERAP1$^{+/+}$RAG2$^{-/-}$ mice were stained with anti-CD8 and anti-Vα2 antibodies and analyzed by flow cytometry. Numbers indicate the percentage of cells within the gated area.

CD8⁺ T cell responses

Finally, we determined the impact of ERAP1 deficiency on the generation of CTL responses in vivo. We loaded splenocytes from TAP1$^{-/-}$ mice ex vivo with OVA by osmotic shock and used these cells to immunize ERAP1$^{-/-}$ or ERAP1$^{+/+}$ mice. 7 d later, mice were tested for the generation of OVA$_{257–264}$-specific CD8 T cell responses by stimulating splenocytes with OVA$_{257–264}$ and measuring the prevalence of IFN-γ–producing CD8^{+} T cells. The results showed a profound defect (three- to fourfold reduction) in the generation of OVA$_{257–264}$-specific CD8^{+} T cell responses in vivo (Fig. 7, A and B).

We also determined the immune response of ERAP1$^{-/-}$ mice to infection by an influenza virus. Mice were infected intranasally with the PR8 strain of influenza virus and, 10 d later, lymph nodes from these animals were stimulated ex vivo with synthetic versions of a panel of H-2K^{b}– and H-2D^{b}–restricted peptide epitopes, and the prevalence of epitope-specific CD8 T cells in the cultures was evaluated by intracellular detection of IFN-γ. Our results revealed moderately reduced responses in the generation of CTL responses directed against several of the immunodominant epitopes; nonetheless, the differences did not reach statistical significance in any single experiment (Fig. 7, C and D).

DISCUSSION

Our findings have revealed an important in vivo role of ERAP1 in optimizing peptides for presentation by MHC class I molecules. Both H-2K^{b} and H-2D^{b} bind with peptides that contain hydrophobic COOH-terminal amino acid residues, which represent preferred substrates for TAP (1, 2) and ERAP1 (24). In addition, both H-2K^{b} and H-2D^{b} can bind with peptides that contain a proline residue in position 3, which are poorly translocated by the TAP peptide transporter (40) and, therefore, would likely be translocated as longer precursors. Consistent with these prior studies, we found that ERAP1 deficiency resulted in a significant reduction in the surface expression of H-2K^{b} and H-2D^{b}. In addition to its effects on class Ia molecules, ERAP1 expression also influenced surface expression of the class Ib molecules Qa-2 and Qa-1^{b}. Consistent with prior studies (19, 21), we found that ERAP1 expression can have a positive, neutral, or negative impact on the presentation of individual class I antigens. For several of the epitopes tested, including H60 (an 8-mer peptide presented by K^{b}), HY (a 9-mer peptide presented by D^{b}), and OVA$_{257–264}$ (an 8-mer peptide presented by K^{b}), ERAP1 expression appeared to play an important role, as presentation of these epitopes by ERAP1$^{-/-}$ cells, compared with ERAP1$^{+/+}$ cells, was reduced 80–90%. These findings indicate that cytosolic proteases are unable to compensate for ERAP1 deficiency in generating physiological levels of some epitopes. Because most minor H antigens and the epitopes recognized by alloreactive, Qa-1^{b}–restricted CTLs are constitutively expressed, cytosolic proteases should have sufficient opportunity to sample peptide precursors derived from these antigens that are recycled between the ER and the cytosol (41, 42). Thus, we conclude that ERAP1 plays a rate-limiting role in the generation of a sizeable subset of peptides for presentation by MHC class I molecules to CTLs. Consistent with this conclusion, we found that ERAP1$^{+/-}$ mice exhibited a phenotype that, at least in some assays, was intermediate between wild-type and mutant animals. Nevertheless, for some epitopes, ERAP1 expression had no effect on antigen presentation (e.g., H4^{b}) or instead suppressed antigen presentation (e.g., H13^{b} and LCMV gp33).

Prior studies have provided conflicting results regarding the role of ERAP1 in controlling MHC class I cell surface expression (19, 21, 22). ERAP1 knockdown by small interfering RNA in murine L cells resulted in decreased expression of both H-2K^{k} and H-2L^{d} (19). Another group of

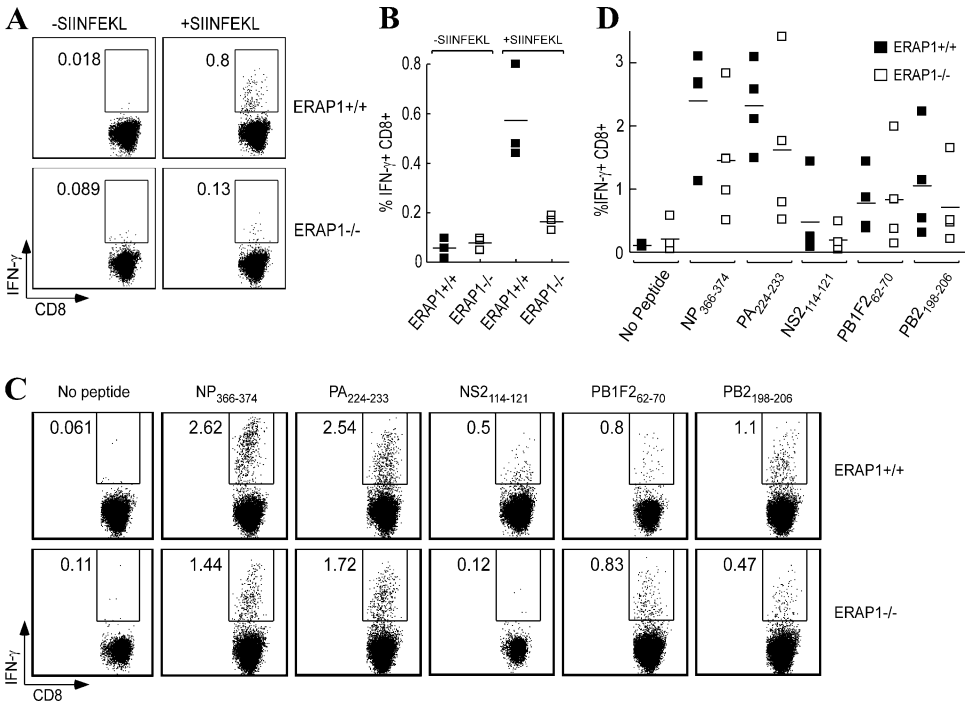

Figure 7. CD8$^+$ T cell responses. (A and B) CTL responses to OVA. The indicated mice were immunized with apoptotic splenocytes from TAP1$^{-/-}$ mice, loaded ex vivo with OVA by osmotic shock. 7 d later, spleen cells from these animals were stimulated with or without $OVA_{257-264}$ peptide for 6 h and IFN-γ–producing CD8$^+$ T cells were detected by flow cytometry. Representative flow cytometry plots (A) and a summary of the percent IFN-γ$^+$CD8$^+$ cells (B) are shown for ERAP1$^{+/+}$ and ERAP1$^{-/-}$ mice ($n = 3$ per group). Numbers indicate the percentage of cells within the gated area. (C and D) CTL responses to influenza virus. Mice were infected intranasally with the PR8 strain of influenza virus. 10 d later, mediastinal lymph node cells of these animals were stimulated in the presence or absence of the indicated peptides for 6 h and IFN-γ–producing CD8$^+$ T cells were detected by flow cytometry as described in Materials and methods. Representative flow cytometry plots (C) and a summary of the percent IFN-γ$^+$CD8$^+$ cells (D) are shown for ERAP1$^{+/+}$ and ERAP1$^{-/-}$ mice ($n = 4$ per group). Numbers indicate the percentage of cells within the gated area.

investigators showed that ERAP1 knockdown in K^b-transfected HeLa cells did not alter K^b surface expression but resulted in an increase in HLA class I surface expression (21). Conversely, ERAP1 overexpression in H-2K^b–transfected COS cells did not affect K^b surface expression but led to significant suppression of monkey class I expression (21). In sharp contrast with the latter studies, a third group of investigators reported that ERAP1 knockdown in HeLa cells resulted in a moderate decrease in HLA class I expression (22). We found that ERAP1 deficiency consistently led to a reduction in the steady-state levels of K^b, D^b, and Qa-2 surface expression. These findings are consistent with prior studies evaluating the effects of ERAP1 knockdown on class I expression in murine cells (19) but only partially agree with studies that have investigated the effects of ERAP1 knockdown or overexpression on H-2K^b expression in HeLa cells and COS cells, respectively (21).

Prior studies regarding the effects of IFN-γ on class I surface expression have also provided conflicting results. One group of investigators reported that ERAP1 gene silencing in H-2K^b–transfected HeLa cells treated with IFN-γ resulted in significant suppression of both surface K^b and HLA expression (21). However, another group of investigators reported that ERAP1 silencing in IFN-γ–treated HeLa cells resulted only in a slight diminution in HLA class I expression, which was less evident than the decrease in class I expression caused by ERAP1 silencing in untreated cells (22). Consistent with the latter studies, we found that differences in class I surface expression were less evident in splenocytes and fibroblasts treated with IFN-γ and in Con A–activated T lymphocytes. Moreover, we found a slight but reproducible defect in the surface stability of K^b and D^b molecules on nonstimulated splenocytes from ERAP1 mutant mice but were unable to detect defects in class I maturation or stability in ERAP1$^{-/-}$ Con A blasts. Collectively, our findings suggest that ERAP1 plays a more important role in generating class I–binding peptides during steady-state than during conditions where IFN-γ is produced. These findings were surprising because ERAP1 expression itself is profoundly induced by IFN-γ (21). One possibility is that induction of ERAP1 expression during IFN-γ treatment results in increased epitope destruction compared with the levels of epitope destruction in the absence of IFN-γ. Nevertheless, our antigen presentation and immunization studies revealed a critical role of ERAP1 for presenting individual peptides to CD8$^+$ T cells in both the absence and presence of IFN-γ production. Thus, ERAP1 significantly impacts the presentation of individual peptides but has only relatively modest effects on the overall capacity

of the generated peptide pool to stabilize class I molecules, particularly when IFN-γ is produced. This conclusion is consistent with the idea that ERAP1 can both enhance and limit antigen presentation of individual peptide epitopes (21).

Although differences between our studies and those of Serwold et al. (19) and Saveanu et al. (22) with the report by York et al. (21) remain unclear, it is possible that the immortalized cell lines used by the latter group of investigators expressed nonphysiological levels of antigen-processing molecules. For example, differences in the expression levels of human ERAP2 among the HeLa cell lines analyzed by Saveanu et al. and York et al. have been noted (9).

Our studies with Qa-2 and Qa-1^b molecules provide the first direct evidence for a role of ERAP1 in generating peptides for surface display by class Ib molecules. Qa-2 antigens are encoded by several class Ib genes and are either linked to the cell membrane via glycosylphosphatidylinositol anchors or secreted from cells (43). Qa-2 binds with a large array of nonameric peptides with a unique motif containing histidine at position 7 (29, 30, 44). Expression of both secreted and glycosylphosphatidylinositol-bound Qa-2 molecules is dependent on a functional TAP peptide transporter (45), and we show here a role of ERAP1 for steady-state levels of Qa-2 surface expression, suggesting that most peptides loaded onto Qa-2 molecules are generated via the conventional class Ia antigen-processing pathway. In sharp contrast with Qa-2, Qa-1^b binds with a highly restricted set of nonameric peptides (31). Qa-1^b predominantly binds with a single peptide, Qa-1 determinant modifier (Qdm), derived from the leader sequence of other class I molecules (31, 46). Despite its localization within a signal sequence, presentation of Qdm on Qa-1^b is dependent on both TAP (47) and Tapasin (48). The production of Qdm requires several antigen-processing events. After biosynthesis and entry of the nascent class I heavy chain into the ER, the signal sequence is cleaved by signal peptidase. The resulting 24–amino acid Qdm peptide precursor, which is embedded in the membrane, is then cleaved by signal peptide peptidase, which allows the release of the NH_2-terminal peptide fragment into the cytosol. This fragment, MGAMAPRTLLLLLA (Qdm is underlined), is then processed by cytosolic proteases to generate the final COOH terminus (current evidence suggests that the proteasome is not involved), resulting in a Qdm precursor containing a two–amino acid NH_2-terminal extension (46). Here, we demonstrate that ERAP1 expression enhances the presentation of Qdm to Qdm-dependent, Qa-1^b–restricted CTLs, suggesting that ERAP1 contributes to the removal of the two NH_2-terminal amino acids of this peptide precursor. This conclusion is consistent with a prior study demonstrating that a Qdm precursor with a two–amino acid NH_2-terminal extension can be processed to generate the Qdm epitope in the ER of TAP-deficient cells (49). However, we found that the reactivity of CTL clones with ERAP1-deficient cells was only partially diminished, suggesting that cytosolic aminopeptidases can trim this Qdm peptide precursor as well, in a manner that is partially redundant with ERAP1. Nevertheless, it remains possible that during certain infections or in cancer cells, ERAP1 expression may represent a rate-limiting step in presenting Qdm peptides to Qa-1^b–restricted CTLs or natural killer cells expressing CD94/NKG2 receptors.

Although our studies with Qdm indicate a critical role of ERAP1 for the processing of signal sequence–derived peptide epitopes, they do not preclude the possibility that some signal sequences can be processed independently of ERAP1. Indeed, presentation of LCMV gp33, which is contained within the signal sequence of the viral glycoprotein (50), to gp33-specific, D^b-restricted T cells, was enhanced in ERAP1-deficient cells, despite the requirement of TAP (51) and the proteasome (52) in the processing of this epitope. These findings suggest that ERAP1 normally plays a role in destroying the LCMV gp33 epitope. In future studies, it will be interesting to infect mutant mice with LCMV and determine the strength of the CD8$^+$ T cell response directed against the gp33 and other LCMV epitopes.

A particularly surprising result of our studies was that, at least in some assays, ERAP1$^{+/-}$ mice exhibited a phenotype that was intermediate between ERAP1$^{+/+}$ and ERAP1$^{-/-}$ mice. To our knowledge, this has not been described for any other mutations that affect the class I antigen presentation pathway. However, an intermediate phenotype, at least with respect to some aspects of antigen presentation, has been described for mice with a heterozygous mutation in the class II peptide exchange factor H-2DM (53). Thus, ERAP1 may play a rate-limiting role in the generation of a sizable subset of peptide epitopes. Although currently unclear, the differential effects of ERAP1 heterozygozity on the processing of individual epitopes likely depends on the dose of the antigen, the method of antigen introduction, the length of antigen incubation with APC, and/or the sensitivity of the read-out assay.

In conclusion, our findings have revealed an important in vivo role of ERAP1 in controlling antigen presentation by both class Ia and class Ib molecules. We demonstrated that ERAP1 expression can have a positive, neutral, or negative contribution in the generation of individual class I epitopes. Additional studies with these animals will be helpful in elucidating the role of ER-associated peptidase activity in the development of antiviral immune responses and in regulating the immunodominance hierarchy of CD8$^+$ T cell responses in vivo.

MATERIALS AND METHODS

Mice. C57BL/6 mice were obtained from The Jackson Laboratory and 129S6/SvEvTac mice were obtained from Taconic. TAP1-deficient mice (32) and Tapasin-deficient mice (33) have been described. P14^{Tg}RAG2$^{-/-}$ mice were obtained from Taconic and were bred with ERAP1 mutant mice to obtain P14^{Tg}ERAP1$^{-/-}$RAG2$^{-/-}$ and P14^{Tg}ERAP1$^{+/+}$RAG2$^{-/-}$ mice. OT-1^{Tg} mice and RAG1$^{-/-}$ mice were obtained from The Jackson Laboratory and bred to obtain OT-1^{Tg}RAG1$^{-/-}$ mice. Mice were maintained in accordance with the Institutional Animal Care and Use Committee at Vanderbilt University.

Generation of ERAP1 mutant mice. To establish an ERAP1 targeting construct, a 5.4-kb XhoI–ClaI fragment from the 5′ end of the ERAP1 gene (from exon 2 to intron 4) and a 5.3-kb NotI–SacII fragment from

the 3′ end of ERAP1 (from the 3′ end of exon 6 to exon 11) were amplified from 129S6/SvEvTac genomic DNA with Pfu Ultra DNA polymerase (Stratagene) by PCR (primers for amplification of the 5′ fragment: forward primer 5′-AACACTCGAGATACTTGCAGCAACACAGTTTGAACCCACAGCTG-3′ and reverse primer 5′-GTGAATCGATGCTTACTAGATGCAGAAGACTTTTCTTTATCGT-3′; primers for amplification of the 3′ fragment: forward primer 5′-ATGAGCGGCCGCTGCCAAATTTATGGAGTTTGTGTCTGTCACTGTG-3′ and reverse primer 5′-TTAACCGCGGTTCAGCAAAAATCTCTGGACTGAGTCTGATT-3′). These DNA fragments, a neomycin resistance cassette (Neo), and a thymidine kinase cassette (TK) were assembled in a pBluescript II vector (Stratagene) to generate the targeting vector. The Neo cassette replaces a fragment from intron 4 up to the 5′ end of exon 6, which contains the sequence encoding the Zinc-binding motif in the putative active site of ERAP1. Strain 129S6/SvEvTac-derived embryonic stem (ES) cells (TL-1; obtained from B. Hogan, Duke University Medical Center, Durham, NC) were transfected with the KpnI-linearized targeting vector. G418-resistant colonies were selected and isolated as described previously (32). Genomic DNA from individual clones was digested with EcoRV and hybridized with 5′- and 3′-flanking probes (Fig. 1 A), which were generated by PCR amplification (primers for amplification of the 5′ probe: forward primer 5′-TAAGGTTACAACTGCATGTCTTCATAC-3′ and reverse primer 5′-AAACTGTGTTGCTGCAAGTATTCTAC-3′; primers for amplification of the 3′ probe: forward primer 5′-AGTTTCTACAAAACACAAATGATCTCC-3′ and reverse primer 5′-CTGTTTTCAGAAATAAACCACAACTTT-3′). Chimeric mice were generated as described previously (32), mated with C57BL/6 or 129S6/SvEvTac mice, and scored for germline transmission. Mice were genotyped by digestion of genomic DNA with EcoRV, followed by hybridization with one or both probes described above.

Analysis of ERAP1 expression by RT-PCR and immunoblotting. For RT-PCR analysis, total RNA treated with RQ1 RNase-free DNase (Promega) was subjected to reverse transcription (Advantage RT-for-PCR kit; CLONTECH Laboratories, Inc.) and cDNA was amplified by PCR with Taq polymerase (Promega). ERAP1 mRNA was amplified using forward (5′-CACTGTGAAGATGAGTACCTAC-3′) and reverse (5′-GTGTGGATACAGGGTGAGAG-3′) primers, flanking the deleted ERAP1 gene fragment, which produces a 551-bp fragment in wild-type animals. β-actin mRNA was amplified as a control using published primers (54).

For Western blot analysis, the rough ER from the liver was isolated as described previously (55) and the lumenal fraction was separated on 6% SDS-PAGE gels. Immunoblotting was performed with a rabbit antiserum raised against a peptide (QNSDIESLKASNGD) from the NH_2 terminus of mouse ERAP1 (Cocalico Biologicals, Inc.) or with an anti-gp96 polyclonal antibody (Santa Cruz Biotechnology, Inc.), and then probed with horseradish peroxidase–conjugated goat anti–rabbit IgG polyclonal antibody (sc-2054; Santa Cruz Biotechnology, Inc.). Blots were developed using the ECL Plus kit (GE Healthcare).

Isolation of fibroblast cell lines. Ear fibroblast cells derived from ERAP1$^{-/-}$ and ERAP1$^{+/+}$ animals were immortalized by serial passage in vitro.

Flow cytometry. The following mAbs were used for flow cytometry: anti-CD4, anti-CD8α, anti-CD8β, anti-Vα2, anti-B220, anti-CD11b, anti-CD11c, anti–IFN-γ (all from BD Biosciences), anti–H-2K^b (clone Y3; American Type Culture Collection [ATCC]), anti–H-2D^b (clone B22.249; ATCC), anti–Qa-2 (clone 1-2-3; BD Biosciences), anti–Qa-1^b (clone 6A8.6F10.1A6; BD Biosciences), and an antibody (25-D1.16) specific for H-2K^b combined with $OVA_{257–264}$ (provided by A. Porgador [Ben Gurion University of the Negev, Beer Sheva, Israel] via L. Pease [Mayo Clinic College of Medicine, Rochester, MN]; reference 56). Cell suspensions from various tissues were prepared according to standard procedures. In some experiments cells were treated with OVA protein, synthetic peptides, recombinant mouse IFN-γ (BD Biosciences), Con A (Calbiochem), or brefeldin A (Sigma-Aldrich) before staining. Cells were stained by incubation with antibody at 4°C for 1 h followed by three washes in cold PBS supplemented with 1% fetal calf serum and 0.05% NaN_3. For unconjugated primary antibodies, the samples were then incubated with a fluorescently labeled secondary antibody and washed three times. After the final wash, cells were analyzed using a FACSCalibur Flow System (Becton Dickinson) and data were analyzed using FlowJo software (TreeStar). Dead cells were excluded from the analysis based on their forward and sideway light scattering properties.

MHC class I maturation and thermostability assays. MHC class I maturation was examined with a modified pulse-chase and immunoprecipitation procedure (32). Con A–induced T cell lymphoblasts were starved for 1 h in methionine/cysteine-free RPMI 1640 medium (Mediatech) at 10^7 cells/ml, and then pulsed with 500 μCi/ml of a [^{35}S]methionine/cysteine mix (MP Biomedicals, Inc.) for 10 min at 37°C. After removal of one seventh of the cells for the 0 time point, the remaining cells were washed with complete RPMI 1640 medium supplemented with 10% fetal calf serum and 1 mM methionine and 1 mM cysteine, and further incubated in the same medium at 37°C. Cell aliquots were removed at different time points, spun through cold PBS, and stored at −20°C. Cells were lysed in 50 mM Tris-Cl, pH 7.4, 5 mM $MgCl_2$, 0.5% NP-40 (Fluka), and 1 mM PMSF (Sigma-Aldrich). After removal of insoluble materials, the lysates were precleared with normal mouse serum and immunoprecipitated with conformation-dependent anti–H-2K^b (Y3) and anti–H-2D^b (B22.249) antibodies. Immunoprecipitates were treated with Endo H (New England Biolabs, Inc.) at 37°C for 1 h before separation by SDS-PAGE. Precipitates were visualized by phosphorimaging and band intensities were quantified with ImageQuant software (Applied Biosystems).

The thermostability of MHC class I complexes in cell extracts was examined as described previously (32, 35). Con A–induced T cell lymphoblasts were labeled with [^{35}S]methionine/cysteine as described above for 1 h, and then washed with RPMI 1640 medium supplemented with 10% fetal calf serum and 1 mM methionine and 1 mM cysteine, and further incubated in the same medium for 2 h at 37°C. Cell lysates, generated as described above, were precleared with normal mouse serum, divided into six parts, and incubated at either 4, 15, 26, 37, 42, or 50°C for 1 h. MHC class I complexes were then precipitated with conformation-dependent anti–H-2K^b (Y3) or anti–H-2D^b (B22.249) antibodies at 4°C. Immunoprecipitates were treated with Endo H at 37°C for 1 h before separation by SDS-PAGE.

Thermostability of surface class I molecules was examined by culturing splenocytes with 10 μg/ml brefeldin A and staining samples after different time points with conformation-dependent anti–H-2K^b (Y3) or anti–H-2D^b (B22.249) antibodies followed by flow cytometry. Data are plotted as the relative amount of class I expression with the 0 time point indicated as 100%.

In vitro antigen processing and presentation assays. To evaluate the presentation of minor H antigens, spleen cells from male ERAP1$^{+/+}$ or ERAP1$^{-/-}$ mice on a homogeneous 129S6/SvEvTac background were used as stimulators for activation of minor H antigen-specific CTL clones, as described previously (38). The following CTL clones were used: SP/H60 and B6-1/H60, specific for H60 presented by H-2K^b; B10/21M-9 and B10/21M-11, specific for H4^b presented by H-2K^b; B/NX-3, specific for H13^b presented by H-2D^b; CTL-10, specific for HY presented by H-2D^b; and 21M/RC6, specific for H4^a presented by H-2K^b (36–38). Spleen cells from female C57BL/6 mice were used as a control. Stimulators ($1–10 \times 10^5$ cells/well) and responders (10^6 cells/well) were cocultured for 1 h, after which 10 μg/ml brefeldin A was added to the medium and cells were incubated for an additional 5 h. Cells were then surface stained with anti-CD8α mAb, washed, permeabilized with the Cytofix/Cytoperm kit (BD Biosciences), stained with anti–IFN-γ, and analyzed by flow cytometry. Data are plotted as percentage CD8$^+$IFN-γ$^+$ cells and normalized to the response against ERAP1$^{+/+}$ cells.

The anti–Qa-1^b-specific CTL clones (obtained from C. Aldrich [Indiana University School of Medicine, Evansville, IN], J. Forman [University of Texas Southwestern Medical Center, Dallas, TX], and M. Soloski [Johns Hopkins University, Baltimore, MD]) were generated from B6.Tla^a (H-2^b and Qa-1^a) anti-C57BL/6 (H-2^b and Qa-1^b) or B10.BR (H-2^k and Qa-1^a) anti-C3H/HeJ (H-2^k and Qa-1^b) mixed lymphocyte cultures (47, 57).

Cytotoxic activity was measured in a standard 4-h ^{51}Cr-release assay (32) using Con A–activated lymphoblast target cells. As a control, cells were incubated with 100 μM Qdm peptide (AMAPRTLLL; Biosynthesis) during labeling. Results are presented as percentage of specific lysis: [(sample release − spontaneous release)/(maximal release − spontaneous release)] × 100.

Presentation of OVA antigens was tested by the loading of bone marrow–derived DCs, generated as described previously (58), or LPS-activated splenocytes with OVA by osmotic shock, as described previously (59). In brief, ~1.5×10^8 cells were incubated in 1 ml of hypertonic medium (0.5 M sucrose, 10% wt/vol PEG 1000, and 10 mM Hepes in RPMI 1640, pH 7.2) containing 10 mg/ml OVA (Sigma-Aldrich) for 10 min at 37°C. 13 ml of prewarmed hypotonic medium (40% H_2O, 60% RPMI 1640) was added and the cells were incubated for an additional 2 min at 37°C. The cells were then centrifuged, washed twice with complete medium, and resuspended in the same medium. One third of the cells was removed immediately at the 0 time point. The remaining cells were further incubated in the same medium at 37°C for 2 or 5 h. Cells loaded with 1 μM $OVA_{257–264}$ peptide (SIINFEKL; Biosynthesis) were cultured for 5 h and used as a positive control. Cell surface expression of H-2K^b/SIINFEKL was examined by flow cytometry with the 25-D1.16 mAb. Alternatively, OVA-loaded cells ($1–2 \times 10^6$) were cultured with 5×10^5 B3Z hybridoma cells (obtained from N. Shastri, University of California, Berkeley, CA; reference 60) overnight and IL-2 in the supernatant was measured by ELISA. For presentation of bacterial-encoded OVA, we infected thioglycolate-elicited peritoneal macrophages (2×10^6 cells) with a recombinant strain of *Listeria monocytogenes* expressing OVA (2×10^8 CFU; obtained from H. Shen, University of Pennsylvania School of Medicine, Philadelphia, PA) in PBS for 30 min. After infection, macrophages were recovered by incubation with 10 mM EDTA in PBS for 1 h. 5×10^4 cells were then cocultured with 2×10^5 nonadherent cells from the spleen and lymph nodes of OT-1^{Tg}RAG1$^{-/-}$ mice for 24 h, and IL-2 in the supernatant was assayed by ELISA. In the cross-presentation assay, splenic DCs were incubated with 1.5 μm latex beads (Polyscience), coated with BSA or OVA by passive adsorption (incubation with beads at 10 mg/ml in 0.1 M borate buffer for 48 h at 4°C, followed by extensive washes) for 48 h, and then cultured with nonadherent splenocytes from OT-1^{Tg}RAG1$^{-/-}$ mice for 24 h, after which the culture supernatant was collected and analyzed for IL-2 content by ELISA.

Presentation of LCMV antigens was determined by infection of bone marrow–derived or splenic DCs with the Armstrong strain (obtained from R. Brutkiewicz, Indiana University School of Medicine, Indianapolis, IN) at 1 PFU/cell. Cells were then cocultured with nonadherent splenocytes from P14^{Tg}RAG2$^{-/-}$ mice for 24 h, and IL-2 in the supernatant was determined by ELISA.

CD8$^+$ T cell responses. For measurement of OVA-specific CD8$^+$ T cell responses, splenocytes from TAP1$^{-/-}$ mice were loaded with 10 mg/ml OVA by osmotic shock as described above, and 2×10^7 cells were injected into ERAP1$^{-/-}$ or ERAP1$^{+/+}$ mice. 7 d later, mice were killed, splenocytes were cultured with 1 μM $OVA_{257–264}$ peptide for 6 h, and intracellular production of IFN-γ by CD8$^+$ T cells was detected by flow cytometry.

To determine immune responses to influenza virus, mice were infected intranasally with 2.5×10^3 PFU of PR8 virus (obtained from H.-G. Ljunggren, Karolinska Institute, Stockholm, Sweden). Mediastinal lymph nodes from infected mice were harvested 10 d later, and cells were cultured in the absence or presence (1 μM) of synthetic versions of the H-2D^b–restricted peptide epitopes $NP_{366–374}$ (ASNENMETM), $PA_{224–233}$ (SSLENFRAYV), or $PB1F2_{62–70}$ (LSLRNPILV), and the H-2K^b–restricted peptide epitopes $NS2_{114–121}$ (RTFSFQLI) or $PB2_{198–206}$ (ISPLMVAYM). 6 h later, IFN-γ production by CD8$^+$ T cells was determined by flow cytometry.

We thank Drs. Carla Aldrich, Randy Brutkiewicz, James Forman, Brigid Hogan, Hans-Gustaf Ljunggren, Larry Pease, Angel Porgador, Nilabh Shastri, Hao Shen, and Mark Soloski for providing various reagents; Tiffaney Vincent, Jie Wei, Dr. Lan Wu, and Shari Roopenian for technical assistance; and Drs. Ian York and Kenneth Rock for sharing information before publication.

This work was supported by National Institutes of Health grants HL68744 (to L. Van Kaer), HL054977 (to S. Joyce), and AI28802 (to D.C. Roopenian).

The authors have no conflicting financial interests.

Submitted: 14 November 2005
Accepted: 1 February 2006

REFERENCES

1. Heemels, M.T., and H. Ploegh. 1995. Generation, translocation, and presentation of MHC class I-restricted peptides. *Annu. Rev. Biochem.* 64:463–491.
2. Pamer, E., and P. Cresswell. 1998. Mechanisms of MHC class I-restricted antigen processing. *Annu. Rev. Immunol.* 16:323–358.
3. Van Kaer, L. 2002. Major histocompatibility complex class I-restricted antigen processing and presentation. *Tissue Antigens.* 60:1–9.
4. Cresswell, P., A.L. Ackerman, A. Giodinin, D.R. Peaper, and P.A. Wearsch. 2005. Mechanisms of MHC class I-restricted antigen processing and cross-presentation. *Immunol. Rev.* 207:145–157.
5. Rammensee, H.G. 1995. Chemistry of peptides associated with MHC class I and class II molecules. *Curr. Opin. Immunol.* 7:85–96.
6. Rock, K.L., and A.L. Goldberg. 1999. Degradation of cell proteins and the generation of MHC class I-presented peptides. *Annu. Rev. Immunol.* 17:739–779.
7. Shastri, N., S. Schwab, and T. Serwold. 2002. Producing nature's gene-chips: the generation of peptides for display by MHC class I molecules. *Annu. Rev. Immunol.* 20:463–493.
8. Yewdell, J.W., E. Reits, and J. Neefjes. 2003. Making sense of mass destruction: quantitating MHC class I antigen presentation. *Nat. Rev. Immunol.* 3:952–961.
9. Saveanu, L., O. Carroll, Y. Hassainya, and P. van Endert. 2005. Complexity, contradictions, and conundrums: studying post-proteasomal proteolysis in HLA class I antigen presentation. *Immunol. Rev.* 207:42–59.
10. Kisselev, A.F., T.N. Akopian, K.M. Woo, and A.L. Goldberg. 1999. The sizes of peptides generated from protein by mammalian 26 and 20 S proteasomes. Implications for understanding the degradative mechanism and antigen presentation. *J. Biol. Chem.* 274:3363–3371.
11. Toes, R.E., A.K. Nussbaum, S. Degermann, M. Schirle, N.P. Emmerich, M. Kraft, C. Laplace, A. Zwinderman, T.P. Dick, J. Muller, et al. 2001. Discrete cleavage motifs of constitutive and immunoproteasomes revealed by quantitative analysis of cleavage products. *J. Exp. Med.* 194:1–12.
12. Cascio, P., C. Hilton, A.F. Kisselev, K.L. Rock, and A.L. Goldberg. 2001. 26S proteasomes and immunoproteasomes produce mainly N-extended versions of an antigenic peptide. *EMBO J.* 20:2357–2366.
13. Rock, K.L., I.A. York, and A.L. Goldberg. 2004. Post-proteasomal antigen processing for major histocompatibility complex class I presentation. *Nat. Immunol.* 5:670–677.
14. Kloetzel, P.M., and F. Ossendorp. 2004. Proteasome and peptidase function in MHC-class-I-mediated antigen presentation. *Curr. Opin. Immunol.* 16:76–81.
15. Knuehl, C., P. Spee, T. Ruppert, U. Kuckelkorn, P. Henklein, J. Neefjes, and P.M. Kloetzel. 2001. The murine cytomegalovirus pp89 immunodominant H-2L^d epitope is generated and translocated into the endoplasmic reticulum as an 11-mer precursor peptide. *J. Immunol.* 167:1515–1521.
16. Momburg, F., J. Roelse, G.J. Hammerling, and J.J. Neefjes. 1994. Peptide size selection by the major histocompatibility complex–encoded peptide transporter. *J. Exp. Med.* 179:1613–1623.
17. Snyder, H.L., J.W. Yewdell, and J.R. Bennink. 1994. Trimming of antigenic peptides in an early secretory compartment. *J. Exp. Med.* 180:2389–2394.
18. Elliott, T., A. Willis, V. Cerundolo, and A. Townsend. 1995. Processing of major histocompatibility class I–restricted antigens in the endoplasmic reticulum. *J. Exp. Med.* 181:1481–1491.
19. Serwold, T., F. Gonzalez, J. Kim, R. Jacob, and N. Shastri. 2002. ERAAP customizes peptides for MHC class I molecules in the endoplasmic reticulum. *Nature.* 419:480–483.
20. Saric, T., S.C. Chang, A. Hattori, I.A. York, S. Markant, K.L. Rock, M. Tsujimoto, and A.L. Goldberg. 2002. An IFN-γ-induced aminopeptidase in the ER, ERAP1, trims precursors to MHC class I-presented peptides. *Nat. Immunol.* 3:1177–1184.
21. York, I.A., S.-C. Chang, T. Saric, J.A. Keys, J.M. Favreau, A.L. Goldberg, and K.L. Rock. 2002. The ER aminopeptidase ERAP1

enhances or limits antigen presentation by trimming epitopes to 8-9 residues. *Nat. Immunol.* 3:1177–1184.
22. Saveanu, L., O. Carroll, V. Lindo, M. Del Val, D. Lopez, Y. Lepelletier, F. Greer, L. Schomburg, D. Fruci, G. Niedermann, and P.M. van Endert. 2005. Concerted peptide trimming by human ERAP1 and ERAP2 aminopeptidase complexes in the endoplasmic reticulum. *Nat. Immunol.* 6:689–697.
23. Serwold, T., S. Gaw, and N. Shastri. 2001. ER aminopeptidases generate a unique pool of peptides for MHC class I molecules. *Nat. Immunol.* 2:644–651.
24. Chang, S.-C., F. Momburg, N. Bhutani, and A.L. Goldberg. 2005. The ER aminopeptidase, ERAP1, trims precursors to lengths of MHC class I peptides by a "molecular ruler" mechanism. *Proc. Natl. Acad. Sci. USA.* 102:17107–17112.
25. Judge, A.D., V. Sood, J.R. Shaw, D. Fang, K. McClintock, and I. MacLachlan. 2005. Sequence-dependent stimulation of the mammalian innate immune response by synthetic siRNA. *Nat. Biotechnol.* 23:457–462.
26. Miyashita, H., T. Yamazaki, T. Akada, O. Niizeki, M. Ogawa, S. Nishikawa, and Y. Sato. 2002. A mouse orthologue of puromycin-insensitive leucyl-specific aminopeptidase is expressed in endothelial cells and plays an important role in angiogenesis. *Blood.* 99:3241–3249.
27. Cui, X., F.N. Rouhani, F. Hawari, and S.J. Levine. 2003. An aminopeptidase, ARTS-1, is required for interleukin-6 receptor shedding. *J. Biol. Chem.* 278:28677–28685.
28. Cui, X., F.N. Rouhani, F. Hawari, and S.J. Levine. 2003. Shedding of the type II IL-1 decoy receptor requires a multifunctional aminopeptidase, aminopeptidase regulator of TNF receptor type 1 shedding. *J. Immunol.* 171:6814–6819.
29. Rotzschke, O., K. Falk, S. Stevanovic, B. Grahovac, M.J. Soloski, G. Jung, and H.G. Rammensee. 1993. Qa-2 molecules are peptide receptors of higher stringency than ordinary class I molecules. *Nature.* 361:642–644.
30. Joyce, S., P. Tabaczewski, R.H. Angeletti, S.G. Nathenson, and I. Stroynowski. 1994. A nonpolymorphic major histocompatibility complex class Ib molecule binds a large array of diverse self-peptides. *J. Exp. Med.* 179:579–588.
31. DeCloux, A., A.S. Woods, R.J. Cotter, M.J. Soloski, and J. Forman. 1997. Dominance of a single peptide bound to the class Ib molecule Qa-1^b. *J. Immunol.* 158:2183–2191.
32. Van Kaer, L., P.G. Ashton-Rickardt, H.L. Ploegh, and S. Tonegawa. 1992. TAP1 mutant mice are deficient in antigen presentation, surface class I molecules, and $CD4^-8^+$ T cells. *Cell.* 71:1205–1214.
33. Grandea, A.G., III, T.N. Golovina, S.E. Hamilton, V. Sriram, T. Spies, R.R. Brutkiewicz, J.T. Harty, L.C. Eisenlohr, and L. Van Kaer. 2000. Impaired assembly yet normal trafficking of MHC class I molecules in Tapasin mutant mice. *Immunity.* 13:213–222.
34. Garbi, N., P. Tan, A.D. Diehl, B.J. Chambers, H.G. Ljunggren, F. Momburg, and G.J. Hammerling. 2000. Impaired immune responses and altered peptide repertoire in tapasin-deficient mice. *Nat. Immunol.* 1:234–238.
35. Williams, A.P., C.A. Peh, A.W. Purcell, J. McCluskey, and T. Elliott. 2002. Optimization of the MCH class I peptide cargo is dependent on tapasin. *Immunity.* 16:509–520.
36. Strausbauch, M.A., W.K. Nevala, D.C. Roopenian, H.E. Stefanski, and P.J. Wettstein. 1998. Identification of mimotopes for the H4 minor histocompatibility antigen. *Int. Immunol.* 10:421–434.
37. King, T.R., G.J. Christianson, M.J. Mitchell, C.E. Bishop, D. Scott, I. Ehrmann, E. Simpson, E.M. Eicher, and D.C. Roopenian. 1994. Deletion mapping by immunoselection against the H-Y histocompatibility antigen further resolves the Sxra region of the mouse Y chromosome and reveals complexity of the Hya locus. *Genomics.* 24:159–168.
38. Choi, E.Y., G.J. Christianson, Y. Yoshimura, T.J. Sproule, N. Jung, S. Joyce, and D.C. Roopenian. 2002. Immunodominance of H60 is caused by an abnormally high precursor T cell pool directed against its unique minor histocompatibility antigen peptide. *Immunity.* 17:593–603.
39. Bevan, M.J., and A.W. Goldrath. 1999. Selecting and maintaining a diverse T-cell repertoire. *Immunity.* 11:183–190.
40. Neefjes, J., E. Gottfried, J. Roelse, M. Gromme, R. Obst, G.J. Hammerling, and F. Momburg. 1995. Analysis of the fine specificity of rat, mouse and human TAP peptide transporters. *Eur. J. Immunol.* 25:1133–1136.
41. Koopmann, J.O., J. Albring, E. Huter, N. Bulbuc, P. Spee, J. Neefjes, G.J. Hammerling, and F. Momburg. 2000. Export of antigenic peptides from the endoplasmic reticulum intersects with retrograde protein translocation through the Sec61p channel. *Immunity.* 13:117–127.
42. Roelse, J., M. Gromme, F. Momburg, G. Hammerling, and J. Neefjes. 1994. Trimming of TAP-translocated peptides in the endoplasmic reticulum and in the cytosol during recycling. *J. Exp. Med.* 180:1591–1597.
43. Stroynowski, I., M. Soloski, M.G. Low, and L. Hood. 1987. A single gene encodes soluble and membrane-bound forms of the major histocompatibility Qa-2 antigen: anchoring of the product by a phospholipid tail. *Cell.* 50:759–768.
44. He, X., P. Tabaczewski, J. Ho, I. Stroynowski, and K.C. Garcia. 2001. Promiscuous antigen presentation by the nonclassical MHC Ib Qa-2 is enabled by a shallow, hydrophobic groove and self-stabilized peptide conformation. *Structure.* 9:1213–1224.
45. Tabaczewski, P., and I. Stroynowski. 1994. Expression of secreted and glycosylphosphatidylinositol-bound Qa-2 molecules is dependent on functional TAP-2 peptide transporter. *J. Immunol.* 152:5268–5274.
46. Rodgers, J.R., and R.G. Cook. 2005. MHC class Ib molecules bridge innate and acquired immunity. *Nat. Rev. Immunol.* 5:459–471.
47. Aldrich, C.J., A. DeCloux, A.S. Woods, R.J. Cotter, M.J. Soloski, and J. Forman. 1994. Identification of a Tap-dependent leader peptide recognized by alloreactive T cells specific for a class Ib antigen. *Cell.* 79:649–658.
48. Li, L., B.A. Sullivan, C.J. Aldrich, M.J. Soloski, J. Forman, A.G. Grandea III, P.E. Jensen, and L. Van Kaer. 2004. Differential requirement for tapasin in the presentation of leader- and insulin-derived peptide antigens to Qa-1^b-restricted CTLs. *J. Immunol.* 173:3707–3715.
49. Bai, A., C.J. Aldrich, and J. Forman. 2000. Factors controlling the trafficking and processing of a leader-derived peptide presented by Qa-1. *J. Immunol.* 165:7025–7034.
50. Buchmeier, M.J., and R.M. Zinkernagel. 1992. Immunodominant T cell epitope from signal sequence. *Science.* 257:1142.
51. Hombach, J., H. Pircher, S. Tonegawa, and R.M. Zinkernagel. 1995. Strictly transporter of antigen presentation (TAP)-dependent presentation of an immunodominant cytotoxic T lymphocyte epitope in the signal sequence of a virus protein. *J. Exp. Med.* 182:1615–1619.
52. Gallimore, A., K. Schwarz, M. van den Broek, H. Hengartner, and M. Groettrup. 1998. The proteasome inhibitor lactacystin prevents the generation of an endoplasmic reticulum leader-derived T cell epitope. *Mol. Immunol.* 35:581–591.
53. Martin, W.D., G.G. Hicks, S.K. Mendiratta, H.I. Leva, H.E. Ruley, and L. Van Kaer. 1996. H2-M mutant mice are defective in the peptide loading of class II molecules, antigen presentation, and T cell repertoire selection. *Cell.* 84:543–550.
54. Podojil, J.R., and V.M. Sanders. 2003. Selective regulation of mature IgG1 transcription by CD86 and β2-adrenergic receptor stimulation. *J. Immunol.* 170:5143–5151.
55. Walter, P., and G. Blobel. 1983. Preparation of microsomal membranes for cotranslational protein translocation. *Methods Enzymol.* 96:84–93.
56. Porgador, A., J.W. Yewdell, Y. Deng, J.R. Bennink, and R.N. Germain. 1997. Localization, quantitation, and in situ detection of specific peptide-MHC class I complexes using a monoclonal antibody. *Immunity.* 6:715–726.
57. Hermel, E., C. Smith, and C.J. Aldrich. 2000. Allogeneic responses to the class Ib antigen Qa1: limited T-cell receptor Vα but not Vβ chain usage. *Immunogenetics.* 51:600–605.
58. Lutz, M.B., N. Kukutsch, A.L. Ogilvie, S. Rossner, F. Koch, N. Romani, and G. Schuler. 1999. An advanced culture method for generating large quantities of highly pure dendritic cells from mouse bone marrow. *J. Immunol. Methods.* 223:77–92.
59. Moore, M.W., F.R. Carbone, and M.J. Bevan. 1988. Introduction of soluble protein into the class I pathway of antigen processing and presentation. *Cell.* 54:777–785.
60. Karttunen, J., S. Sanderson, and N. Shastri. 1992. Detection of rare antigen-presenting cells by the lacZ T-cell activation assay suggests an expression cloning strategy for T-cell antigens. *Proc. Natl. Acad. Sci. USA.* 89:6020–6024.